JOURNAL OF MATERIALS SCIENCE 20 (1985) 2882–2888

Holographic screening method for microelastic solids

R. S. LAKES*, D. GORMAN‡, W. BONFIELD
Department of Materials, and ‡Department of Mechanical Engineering, Queen Mary College, Mile End Road, London E1 4NS, UK

An experimental method is presented for the rapid evaluation of structured solids with microelastic degrees of freedom associated with the microstructure. By contrast with earlier methods based on size effect studies, the present method makes use of a single specimen subjected to holographic interferometry. Results are presented for polymethyl methacrylate and for a dense polyurethane foam, which in previous studies were demonstrated to behave, respectively, as classically elastic and Cosserat solids.

1. Introduction

1.1. Microelastic degrees of freedom: Cosserat model

Structured materials can possess degrees of freedom in addition to those of a homogeneous solid. The degrees of freedom considered here are distinct from phenomena such as viscoelasticity, plasticity, anisotropy, and thermoelasticity. One way to take into account some of the possible motions and deformations of structural elements in a continuum model is to apply the Cosserat (micropolar) theory of elasticity [1–3]. This theory, which includes the ordinary or classical elasticity as a special case, postulates the local rotation of points to be an independent kinematic variable not necessarily equal to the macro-rotation associated with the gradients of the displacements. The local or micro-rotation is associated with a new dynamical variable, the couple per unit area upon a differential element, or couple stress. The constitutive equations for an isotropic Cosserat elastic solid are, for a linear material at small strain [3]:

$$t_{kl} = \lambda e_{rr}\delta_{kl} + (2\mu + \kappa)e_{kl} + \kappa e_{klm}(r_m - \phi_m)$$

$$m_{kl} = \alpha\phi_{r,r}\delta_{kl} + \beta\phi_{k,l} + \gamma\phi_{l,k}$$

in which t_{kl} is the (asymmetric) usual (Cauchy) stress tensor, e_{kl} is the small strain, defined in terms of the displacement u: $e_{kl} = 1/2(u_{k,l} + u_{l,k})$, r is the macro-rotation $r_m = 1/2e_{mln}u_{n,l}$ in which e_{mln} is the permutation symbol. m_{kl} is the couple stress tensor, ϕ is the micro-rotation, and α, β, γ, κ, μ, λ are elastic constants. Classical elasticity is obtained as a special case by allowing the first four of these elastic constants to tend to zero.

Cosserat elastic solids are predicted to differ in many ways from classically elastic materials. In the bending [4] and torsion [5] of rods and in the bending of plates [4] size effects are predicted to occur in which thin specimens are more rigid than expected from the behaviour of thick specimens. Mode structure of vibrating objects is predicted to be modified in such a way that higher modes are shifted to frequencies which exceed their classical values [6, 7]. Perhaps the most important prediction in terms of practical uses of materials is that stress concentration factors around small holes are reduced [8] and that the stress intensity factor associated with cracks can differ substantially with classical predictions [9–11].

1.2. Current experimental methods

Experimental studies have generally be based on the size effects (stiffening) predicted to occur

*Permanent address: Department of Biomedical Engineering, The University of Iowa, Iowa City, Iowa 52242, USA.

0022–2461/85 $03.00 + .12

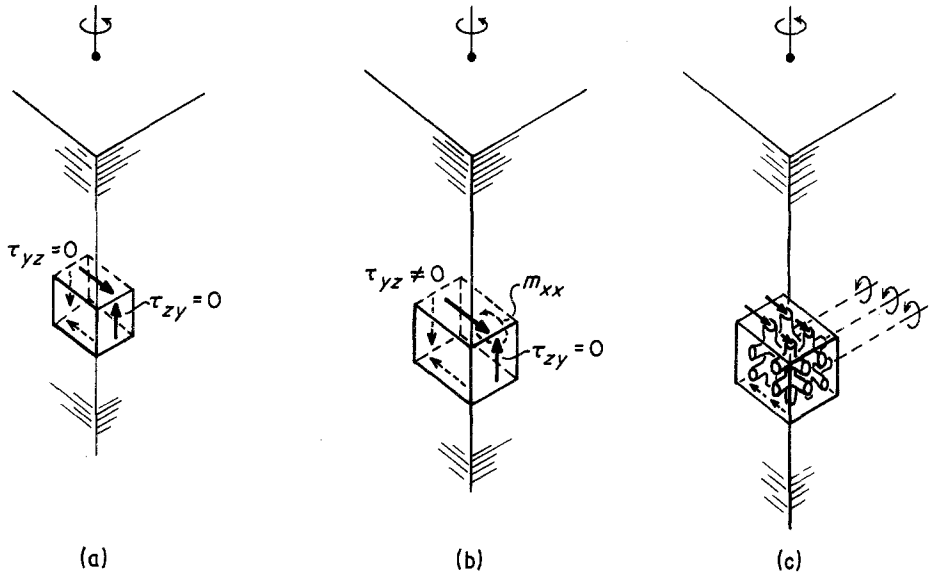

Figure 1 Free-body diagram of corner element. (a) Classically elastic solid. (b) Cosserat elastic solid. (c) A structured solid.

in thin specimens. Plate bending studies of metals [12, 13] and torsion studies of rods of a model composite [5] disclosed classical behaviour, while a thickness-resonance size effect study of a polymer foam [14] disclosed possible effects of Cosserat elasticity. One of the authors (R.L.) has performed torsion and bending size-effect experiments on human compact bone [15–18], a low density polymeric foam [19] a syntactic foam and a high density polymeric foam [20]. Bone behaves as an anisotropic Cosserat solid, the low-density foam is non-classical but appears to require a more complex model than the Cosserat model, the syntactic foam is very nearly classical, and the dense polyurethane foam behaves as an isotropic Cosserat solid for which all six elastic constants are determined.

The method of size effects, then, is capable of distinguishing between classical and Cosserat elastic behaviour and in its more recent forms, is capable of determining all six Cosserat elastic constants of an isotropic material. The method of size effects, however, has the disadvantage that it is extremely tedious: specimens must be cut to progressively smaller sizes or an ensemble of specimens of identical properties must be obtained. In addition, care must be taken that no macroscopic inhomogeneity or variation among specimens is allowed to obtrude in the data in such a way as to mimic a size effect. Also, the range of specimen sizes must include diameters comparable to the length scale of the microstructure. A set of specimens from 5 to 25 times the characteristic length of the microstructure, in diameter will suffice for the demonstration of the existence of microelastic effects, if present. Such a set will also permit a reasonably accurate determination of the Cosserat characteristic lengths [15, 17]. If, however, the structure size is small, the preparation of the thinnest of these specimens can present a significant challenge to the experimentalist. The present experimental method is intended to remedy some of these shortcomings and to provide a rapid screening technique to distinguish classical from Cosserat elastic solids.

2. Prismatic bar in torsion

2.1. Classical and Cosserat elastic analyses: corner elements

Theoretical determination of stress and strain distributions in a prism of square or rectangular cross-section is a well-known problem in classical elasticity [21]. The corresponding problem in Cosserat elasticity is more difficult and has been examined only recently [22]. For the purposes of this article, the behaviour of a small portion of material at a corner of the prism is considered. Fig. 1a shows such a corner element of a classically elastic solid, with surface tractions associated with shear stress indicated. Since there are no loads applied to the lateral surfaces in torsion, the shear stress must be zero at the corner

by virtue of the symmetry of the stress tensor in classical elasticity. Fig. 1b shows a corner element in a Cosserat elastic material. There is still no load on the lateral surface, by assumption. In this case, however, couple stress due to the local rotation gradient is present, as is an asymmetry in the (ordinary) force stress. This asymmetry in the stress satisfies the requirement of equilibrium of the element, since the torque produced by the asymmetric force stress is balanced by the torque due to the couple stress. The conclusions of the above arguments are borne out in the detailed mathematical analyses in [21, 22]. A physical perception of the above may be gained by examination of Fig. 1c, which shows a corresponding corner element in a lattice structure. Each strut in the lattice can support both a force and a moment. For a microelement containing a sufficient number of struts, the average shear force per area can be equated with the shear stress and the average moment per unit area with the couple stress. The diagram then becomes equivalent to Fig. 1b.

2.2. A crack in the corner

The aim of the present experimental method is to reveal the presence or absence of Cosserat elastic effects in the simplest and most graphic manner possible. A small crack or notch is therefore introduced at the corner. In a classical solid there is no stress at the corner, hence no tendency for the crack to open when the bar is subjected to torsion. This is strictly true only for a crack of infinitesimal depth since the shear stress is exactly zero only at the corner itself. In a Cosserat solid, the introduction of the crack will relieve nonzero force stresses and couple stresses, hence the crack will tend to open in mode III as shown in Fig. 2. This nonclassical crack opening is the basis for the present method.

The present method, in contrast to other possible methods based on Cosserat elastic analyses of other crack geometries [9–11], has the advantage that a classical material yields a null result and a Cosserat solid yields a finite result in terms of relative crack displacement.

3. Experimental methods

3.1. Mechanical aspects

Specimens of a prismatic shape with square cross-section were prepared on a milling machine

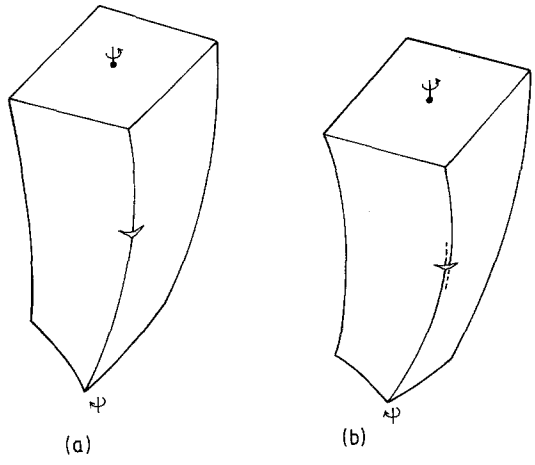

Figure 2 Corner crack in a twisted bar. (a) Classically elastic solid. (b) Cosserat elastic solid.

to give a thickness ~7 to 15 mm and length ~120 mm. Scale marks were made on the surface, which was also coated with a thin layer of reflective paint. Torque was applied to the specimen statically by placing a known weight on a torque arm. The rotating end of the specimen was constrained by a ball bearing.

3.2. Holographic aspects

3.2.1. Apparatus and processing

The holographic apparatus is drawn in Fig. 3. A 5 mW helium–neon laser was used in conjunction with a pneumatic vibration isolation table (Newport Corporation) located in a basement room. The laser beam was passed through a beamspreader and spatial filter and was then collimated. Double exposure holograms were produced as follows. An exposure, typically one second in duration, was made using a camera shutter not in contact with the isolation table. Torque was applied, and the specimen was

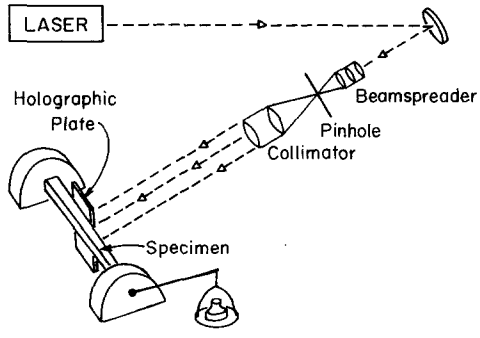

Figure 3 Experimental configuration.

allowed to creep for about 1 min to reduce the creep rate during the second exposure, which was identical in duration to the first. Ostrovsky *et al.* [23] provide an overview of double exposure holography.

The holographic plate, Agfa-Gevaert 8E75HD emulsion, was then removed, developed in Kodak D19 developer for approximately 2 min to a density of ~ 1.6, placed in an acid stopbath for 30 sec, fixed for 2 min, and bleached. Bleach composition was 1.5 g mercuric chloride, 1.5 g potassium bromide, 100 ml water [24]. This bleach is toxic and can be absorbed through the skin, therefore appropriate safety measures including the use of rubber gloves, were taken. The plate was then washed in water for several minutes, and dried in graded alcohols: 50% ethanol for 2 min, 75% ethanol for 2 min, 100% ethanol for 2 min, followed by air drying.

3.2.2. Recording geometry

Fringe patterns observed in double-exposure holographic interferograms depend on the displacement field which occurs between exposures, by virtue of the changes in optical path length which occur. Interpretation of the fringe pattern depends in part upon the geometry in which the hologram is recorded and reconstructed [25] and can be simplified by the choice of an appropriate geometry. In the present experiments the holographic plate was placed parallel to a lateral surface of the specimen, less than 1 mm away. The laser beam was directed at nearly normal incidence to the plate, as shown in Fig. 3. In this configuration, the light passes through the transparent plate, is reflected from the specimen, and enters the plate from the opposite side. A hologram recorded as above and viewed and illuminated in light normally incident to the plate may be interpreted in a particularly simple fashion [25]. The displacement, d, of each point on the specimen in a direction orthogonal to the holographic plate is

$$d = m\lambda/2$$

in which m is the fringe order and λ is the wavelength of laser light used, i.e. 0.6328 μm in this case.

A hologram produced as above, with the references and object light entering the emulsion from opposite sides, is viewed by reflected light. Reconstruction of such a hologram involves Bragg diffraction, which is wavelength sensitive. Consequently, the hologram may be viewed in white light; a laser is not necessary for viewing. The concept is due to Denisyuk [26]. In general, the white light source must be reasonably spatially coherent and this requirement becomes more severe the further the original object was from the hologram plate. In the present approach, the plate is very close to the object and the holograms could be viewed in sunlight or light from an unfrosted incandescent bulb.

Reflected light holograms tend to be very dim unless they are bleached. The bleach process described above converts the amplitude hologram into a phase hologram, considerably improving the diffraction efficiency, and hence the brightness, of the image [24]. Shrinkage of the emulsion during drying can degrade the quality of a reflected light hologram, but the alcohol drying procedure used in this study prevented nonuniformity in drying and improved the image quality [27].

3.2.3. Fringe control

A fringe pattern associated with torsion of a bar of square cross-section is shown in Fig. 4. The twist angle per unit length is 0.033 rad min^{-1}. The right end of the specimen is fixed. The rotation of a cross-section increases with distance from the fixed end and the density of fringes correspondingly increases. Now a rather substantial twist angle per unit length is necessary to reveal mode III opening of a small crack in the corner of the bar. This will result in a dense pattern of fringes, since the crack must be made a sufficient distance from the fixed end such that end effects do not perturb the deformation field near the crack. A variety of "fringe control" methods have been suggested to reduce the density of background fringes in the vicinity of a region of interest [28]. The method used here is to attach the holographic plate to the specimen itself [29]. The plate experiences a rigid body rotation corresponding to the section of the specimen to which it is attached. The point of zero relative motion between plate and specimen, hence a region of low fringe density, is therefore shifted away from the specimen end. Figs. 5 and 6 display fringe patterns obtained by this method. By using this approach, the corner crack can be located away from the specimen end in a region of moderate fringe density, which

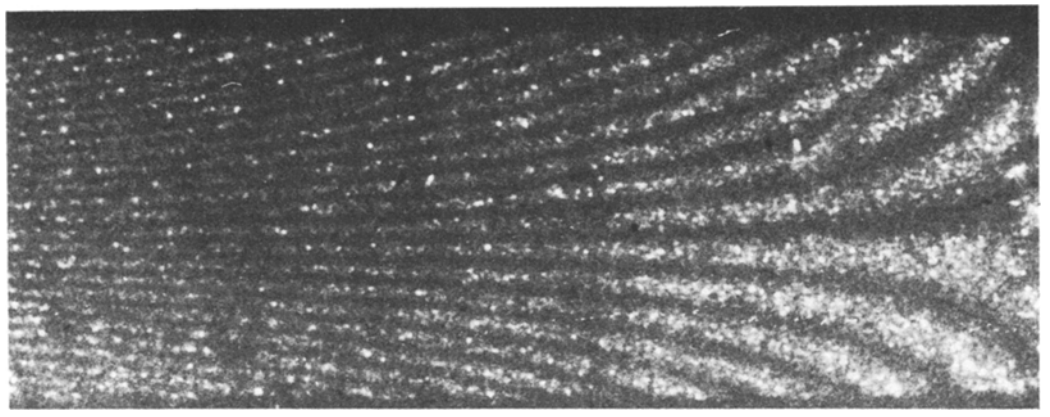

Figure 4 Photograph of a double-exposure hologram of a dense polyurethane foam bar (8.45 mm square cross-section) in torsion. The holographic plate is fixed.

facilitates interpretation of the hologram. In addition to neutralizing the fringe effects of specimen rigid body motions, this approach can eliminate the effect of ambient vibrations, permitting holographic studies in noisy environments [29]. In the present study, the holographic plate was attached to the specimen (i) by cementing with a cyanoacrylate adhesive, and (ii) by a set of steel spring clips. In approach (i) care must be taken not to cement the emulsion side of the plate, and to cement only one or two small points on the specimen. This is accomplished by using one or two thin offsets between plate and specimen. Approach (ii) was simpler, but the size of specimen which could be handled this way was limited.

3.2.4. Photography of holograms

Holograms were illuminated by either the sun or a bare, 1000 W photoflood lamp. Either source

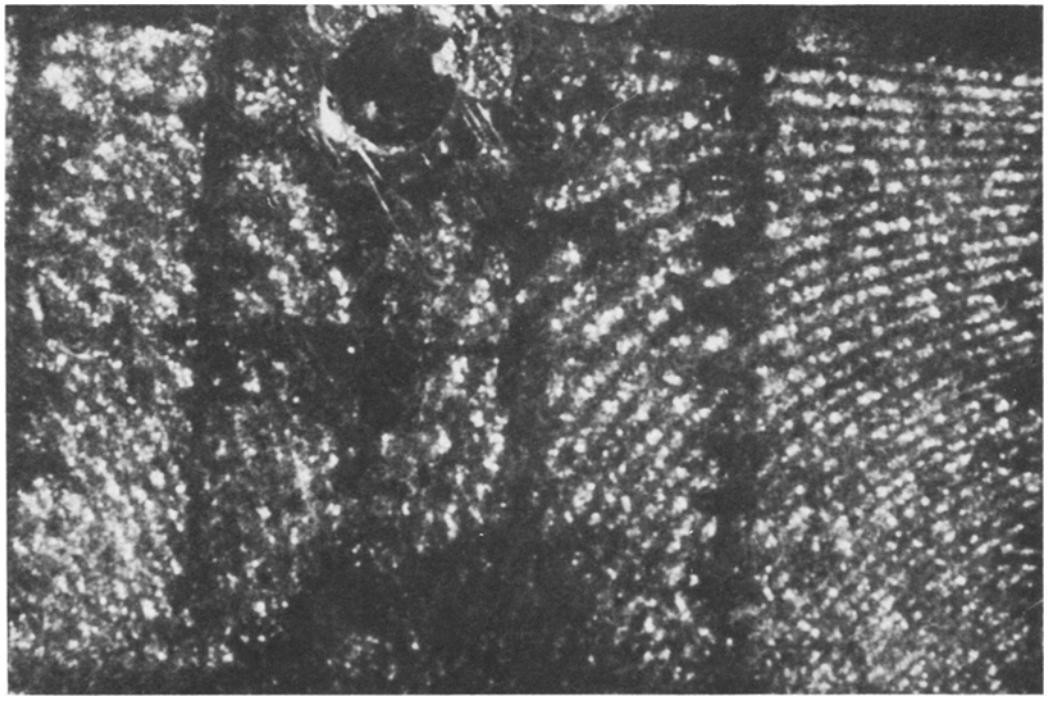

Figure 5 Photograph of a double-exposure hologram of a solid polymethylmethacrylate bar (9.0 mm square cross-section) in torsion, with a crack length of 1.0 mm. The holographic plate is cemented to the bar.

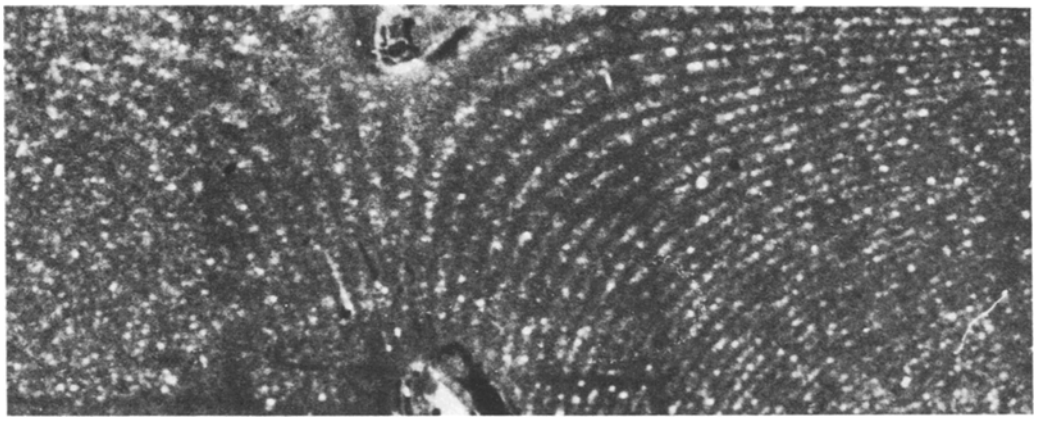

Figure 6 Photograph of a double-exposure hologram of a dense polyurethane foam bar (8.45 mm square cross-section) in torsion, with a crack length of 0.76 mm. The holographic plate is cemented to the bar.

subtends an angle of 0.01 rad at the hologram plate, a sufficiently small angle to prevent blurring of the fringes. The holograms were photographed in 35 mm format, using macro equipment. Since the fringes do not localize at the specimen image surface [25], a small lens aperture was used to obtain sufficient depth of field.

4. Results

4.1. Solid PMMA and foamed polyurethane

A comparison was made between the behaviour of the corner crack in an amorphous material without significant structure at dimensions above the molecular scale, solid polymethyl methacrylate (PMMA), and in a cellular material, a dense ($340\,kg\,m^{-3}$) polyurethane foam with cells from 0.050 to 0.150 mm diameter. Solid PMMA behaves as a classically viscoelastic material [15], while the polyurethane foam behaves as a Cosserat solid [20], as demonstrated by the method of size effects. A holographic fringe pattern for a bar of solid PMMA in torsion is shown in Fig. 5. In this case, the holographic plate was cemented to one point on the specimen, hence the asymmetric pattern. The twist angle per unit length, determined by counting fringes in a manner similar to that used by Wilson [30], was $\theta = 0.14\,rad\,m^{-1}$. The corner crack, exhibits the same fringe order, hence the same displacement, on both sides of the crack. The crack, therefore, has not, within the experimental resolution, opened in mode III. The situation is that of Fig. 2a. In the polyurethane foam, shown in Fig. 6, a shift of about 0.5 fringe between opposite sides of the crack, is visible. One fringe corresponds to half a wavelength of light, or $0.6328\,\mu m/2$. The deformation resembles that shown in Fig. 2b. We define a dimensionless measure of crack opening $u' = u/\theta ac$ so that experiments involving specimens of different cross-section width a, twist angle θ, and crack length c, can be compared. For the polyurethane foam, the maximum corner crack displacement is 1/4 wavelength and $\theta = 0.11\,rad\,m^{-1}$, so $u' = 0.17$. By contrast, in the PMMA, $u' < 0.03$. A finite value of u' is possible in PMMA even though it behaves classically, since the crack length is finite, but no crack opening can be resolved in the PMMA.

The physical significance of the nondimensional displacement u' may be seen in a different perspective if one recalls that the maximum strain γ_{max} in a square classically elastic bar in torsion is $0.675a\theta$ [21]. This strain occurs along the midline of each lateral surface. A "strain" associated with the corner crack opening u may be defined as $\gamma_{cr} = u/c$. Then the ratio of these strains is $\gamma_{cr}/\gamma_{max} = 1.48u'$. The quantity u', then, may be regarded as a measure of the nonclassical corner strain relieved by the crack, normalized to the peak classical strain.

5. Conclusions

A method based on interferometry by reflection holography has been developed for the screening of structured materials for microelastic effects. The presence or absence of mode III opening of a corner crack in a twisted bar, can readily be

judged on the basis of the interferometric fringe pattern.

Polymethylmethacrylate, a material known to be a classical solid, displays zero crack opening, while a dense polyurethane foam identified as a Cosserat solid by the method of size effects, exhibits a finite, observable crack opening.

Acknowledgement

The authors thank the University of Iowa for providing a developmental assignment for R. S. Lakes.

References

1. E. COSSERAT and F. COSSERAT, "Theorie des Corps Deformables" (1909).
2. R. D. MINDLIN, *Int. J. Solids Structures* **1** (1965) 265.
3. A. C. ERINGEN, "Fracture" (Academic Press, New York, 1968) p. 621.
4. G. V. KRISHNA REDDY and N. K. VENKATASUBRAMANIAN, *J. Appl. Mech.* **45** (1978) 429.
5. R. D. GAUTHIER and W. E. JAHSMAN, *ibid.* **42** (1975) 369.
6. R. D. MINDLIN and H. F. TIERSTEN, *Arch. Rat. Mech. Anal.* **11** (1962) 415.
7. A. C. SMITH, *Recent Advances in Engineering Science, II,* **5** (1970) 129.
8. R. D. MINDLIN, *Exp. Mech.* **3** (1963) 1.
9. E. STERNBERG and R. MUKI, *Int. J. Solids Structures* **3** (1967) 69.
10. C. ATKINSON and F. G. LEPPINGTON, *ibid.* **13** (1977) 1103.
11. U. B. C. O. EJIKE, *Int. J. Eng. Sci.* **7** (1969) 947.
12. J. SCHIJVE, *J. Mech. Phys. Solids* **14** (1966) 113.
13. R. W. ELLIS and C. W. SMITH, *Exp. Mech.* **7** (1968) 372.
14. R. W. PERKINS and D. THOMSON, *Amer. Inst. Aeronaut. Astronaut. J.* **11** (1974) 1053.
15. J. F. C. YANG and R. S. LAKES, *J. Biomechanical Eng.* **103** (1981) 275.
16. R. S. LAKES, *ibid.* **104** (1982) 6.
17. J. F. C. YANG and R. S. LAKES, *J. Biomechanics* **15** (1982) 91.
18. R. S. LAKES and J. F. C. YANG, Proceedings of the 18th Midwestern Mechanics Conference – Developments in Mechanics Vol. 12 (1983) p. 239.
19. R. S. LAKES, *J. Mater. Sci.* **18** (1983) 2572.
20. *Idem, Int. J. Solids Structures*, in press.
21. S. P. TIMOSHENKO and J. N. GOODIER, "Theory of Elasticity", 3rd edn. (McGraw-Hill, 1982).
22. H. C. PARK and R. S. LAKES, *Int. J. Eng. Sci.* in preparation.
23. YU. I. OSTROVSKY, M. M. BUTUSOV and G. V. OSTROVSKAYA, "Interferometry by Holography" (Springer-Verlag, Berlin, 1980).
24. J. UPATNIEKS and C. LEONARD, *Appl. Optics* **8** (1969) 85.
25. J. D. BRIERS, *Opt. Quant. Electron.* **8** (1976) 469.
26. Y. DENISYUK, *Sov. Phys. Doklady* **144** (1962) 1275.
27. K. S. PENNINGTON and J. S. HARPER, *Appl. Optics* **9** (1970) 1643.
28. P. M. DELARMINAT and R. P. WEI, *Exp. Mech.* **16** (1976) 241.
29. D. B. NEUMANN and R. C. PENN, *ibid.* **15** (1975) 241.
30. A. D. WILSON, *Appl. Optics* **9** (1970) 2093.

Received 7 September
and accepted 14 September 1984